

# Chirped-pulse interferometry with finite frequency correlations

K.J. Resch,\* R. Kaltenbaek, J. Lavoie, and D.N. Biggerstaff

*Institute for Quantum Computing and Department of Physics & Astronomy,  
200 University Ave. W, Waterloo, N2L 3G1, Canada*

Chirped-pulse interferometry is a new interferometric technique encapsulating the advantages of the quantum Hong-Ou-Mandel interferometer without the drawbacks of using entangled photons. Both interferometers can exhibit even-order dispersion cancellation which allows high resolution optical delay measurements even in thick optical samples. In the present work, we show that finite frequency correlations in chirped-pulse interferometry and Hong-Ou-Mandel interferometry limit the degree of dispersion cancellation. Our results are important considerations in designing practical devices based on these technologies.

## INTRODUCTION

Interference is a fundamental characteristic shared by classical and quantum theories of light, and is used to make the most sensitive measurements of quantities such as distance and time. Although interferometry has long played an important role in physics (eg. from Ref. [1] to Ref. [2]), recent work has raised the question as to how interferometers harnessing quantum effects can provide advantages over purely classical ones. Experiments with entangled photons have demonstrated a wide variety of interference effects that had not previously been seen in classical devices. Prominent examples include automatic dispersion cancellation [3, 4, 5], phase-insensitive interference [6], nonlocal interference [7, 8], ghost imaging [9] & ghost diffraction [10], phase super-resolution [11, 12, 13, 14], and phase super-sensitivity [15, 16].

More recently, there has been an effort to observe analogous effects in classical optical interferometers. Ghost imaging [17, 18], automatic dispersion cancellation [19, 20, 21, 22], phase super-resolution [23], and phase-insensitive interference [21, 24] have been observed in optical systems exploiting purely classical correlations, instead of entanglement. Classical systems have been devised which can exhibit Bell-like correlations, albeit not fulfilling the conditions of a Bell experiment and thus without implications for local hidden variable models [25, 26, 27]. Other methods for dispersion cancellation in classical systems have been described theoretically [28, 29].

From a fundamental perspective this body of work aims to distinguish those cases where quantum effects give a true advantage over classical systems from those where they do not. From a more applied point of view, quantum effects are technically challenging to observe, often requiring generation of fragile entangled states and sensitive detection. Signals are often very weak requiring long integration times. Compounding the last issue, many schemes rely on the correlations in a specific entangled state; one cannot simply increase the number of photons (say by running two entangled states through the interferometer simultaneously) without ruining the requisite quantum correlations. In comparison, many classical schemes offer large signals which are easy to detect, and furthermore can often be increased simply by turning up the power of a laser.

Material dispersion is a limiting issue in low-coherence, or white-light, interferometry. If

dispersive materials are placed in one arm of a two-path interferometer (such as a Michelson interferometer), the resulting interferogram will lose contrast and resolution. In essence, the different frequency components of the white light disagree on when the interferometer path lengths are balanced. The quantum, Hong-Ou-Mandel interferometer (see Fig. 1a) using frequency-entangled photon pairs produces an interferogram that exhibits rather surprising robustness against dispersive broadening. This device relies on frequency-entangled photon pairs. One photon from the pair travels through a dispersive medium, while the other passes through an adjustable delay. After recombination on a 50/50 beamsplitter, the coincidences are recorded as a function of the delay. The coincidence rate shows a dramatic dip when the group delays of the two paths are balanced to within the coherence time of the light. This can be as short as a few fs [30]. Theoretically, the width of the coincidence dip has been shown to be insensitive to all even-orders of dispersion [4]. Experiments have confirmed that the dip is much less susceptible to broadening than white-light interferometry [3]. It has been proposed that optical coherence tomography, a medical imaging technique based on low-coherence interferometry, could benefit from automatic dispersion cancellation [31, 32]. However, the reliance on entangled photons presents a significant barrier to rapid signal acquisition.

We have recently demonstrated an interferometric technique that produces an interferogram with the same advantages as the HOM interferometer with frequency-entangled photon pairs, yet requires no entanglement at all [21]. This technique relies on pairs of classically frequency anticorrelated beams, created by using pairs of oppositely chirped laser pulses. We referred to the device as chirped-pulse interferometry (CPI). A schematic for CPI is shown in Fig. 2a. Pairs of oppositely chirped pulses enter into different input ports of a cross-correlator. As in the HOM, the cross-correlator contains a dispersive element in one arm, and a delay in the other. The intensity of a narrow bandwidth of SFG created in a nonlinear crystal is detected on a standard photodiode. This intensity as a function of delay is the CPI interferogram. In Ref. [21] all of the important features of HOM interference, automatic dispersion cancellation, robustness against loss, phase insensitivity, and enhanced resolution were demonstrated. Furthermore, the signal level measured was roughly seven orders of magnitude larger than that achievable in the quantum device with state-of-the-art photon sources. We have since demonstrated the effectiveness of the device in imaging a multi-interface sample [22]. We have shown that modifications to the device can produce analogous interferometry signatures to quantum beating, the HOM peak, and 2-photon phase super-resolution [24].

Dispersion cancellation in these devices has been described theoretically in the literature [4, 21, 31], but these descriptions assume perfect frequency correlations. Perfect correlations in the HOM interferometer would require down-conversion pump lasers with infinitely narrow spectra, while perfect correlations in CPI would require infinitely long chirped pulses. Of course, these limits are unattainable in practice and here we investigate, theoretically, the limits to dispersion cancellation in the presence of imperfect correlations. The goal of this work is to develop rules of thumb describing the reduction in dispersion sensitivity afforded by a given level of correlation. These considerations will be important in designing practical interferometers which take advantage of dispersion cancellation.

## DISPERSION CANCELLATION IN A HONG-OU-MANDEL INTERFEROMETER WITH FINITE CORRELATIONS

Automatic even-order dispersion cancellation occurs in the two-photon Hong-Ou-Mandel interferometer when the photon pairs are frequency entangled. In the literature [4, 31], the quantum state produced by parametric down-conversion from a narrow band pump laser has been described as,

$$|\psi\rangle = \int d\Omega f(\Omega) |\omega_0 + \Omega\rangle_1 |\omega_0 - \Omega\rangle_2. \quad (1)$$

In this state, the sum of the frequencies of the pair of photons is fixed at  $2\omega_0$  while the individual photons may be individually broadband, depending on the function  $f(\Omega)$ . It has been shown that with such a state, the HOM interference dip is completely insensitive to even-order dispersion. However, this state is an approximation to what can actually be achieved. Any real laser has a finite bandwidth and passes on this frequency uncertainty to the photon pairs.

To obtain some intuition regarding dispersion cancellation with imperfect frequency anticorrelations, we describe the state of a pair of photons with adjustable frequency anticorrelations using,

$$|\psi\rangle = \int d\omega_1 \int d\omega_2 f(\omega_1, \omega_2) |\omega_1\rangle_1 |\omega_2\rangle_2, \quad (2)$$

with the function,  $f(\omega_1, \omega_2)$ ,

$$f(\omega_1, \omega_2) = e^{-\frac{(\omega_1 - \omega_0)^2}{2\sigma^2}} e^{-\frac{(\omega_2 - \omega_0)^2}{2\sigma^2}} e^{-\frac{(\omega_1 + \omega_2 - 2\omega_0)^2}{2\sigma_c^2}}, \quad (3)$$

where  $\sigma$  is the bandwidth of the photons, and  $\omega_0$  the centre frequency. If the photons were created via a parametric down-conversion process, the parameter  $\sigma_c$  plays the role of the bandwidth of the pump laser and controls the strength of the frequency correlations. If  $\sigma_c \gg \sigma$ , then  $f(\omega_1, \omega_2) \approx f_1(\omega_1)f_2(\omega_2)$ , i.e., the bandwidth function is separable and the photons have no frequency correlations. In the opposite limit, where  $\sigma_c \rightarrow 0$  then  $e^{-\frac{(\omega_1 + \omega_2 - 2\omega_0)^2}{2\sigma_c^2}} \rightarrow \delta(\omega_1 + \omega_2 - 2\omega_0)$  and the photons have perfect frequency anti-correlations.

The Hong-Ou-Mandel interferometer is shown in Fig. 1a where a dispersive element is located in one arm. The HOM interference signal is given by the coincidence rate between the two slow square law detectors and is given by,

$$C(\tau) \propto \iint d\omega_1 d\omega_2 |A_{tt}(\omega_1, \omega_2, \tau) + A_{rr}(\omega_1, \omega_2, \tau)|^2, \quad (4)$$

where  $A_{tt}$  ( $A_{rr}$ ) is the amplitude where both photons are transmitted (reflected) at the beamsplitter. These are depicted in Fig. 1b. Here, we are only interested in the width of the HOM interference dip so we ignore the path lengths of the interferometer since they just lead to a time-delay offset. We model the material as subjecting the light to a pure quadratic phase shift  $\phi(\omega) = \epsilon(\omega - \omega_0)^2$ , where  $\epsilon$  is a constant characterizing the strength of the dispersion. Note that we have dropped the group delay term which again just leads to an offset. The amplitudes for the two paths are,

$$A_{tt} = f(\omega_1, \omega_2) e^{i\epsilon(\omega_2 - \omega_0)^2} e^{i\omega_1 \tau} \quad (5)$$

$$A_{rr} = -f(\omega_1, \omega_2) e^{i\epsilon(\omega_1 - \omega_0)^2} e^{i\omega_2 \tau}, \quad (6)$$

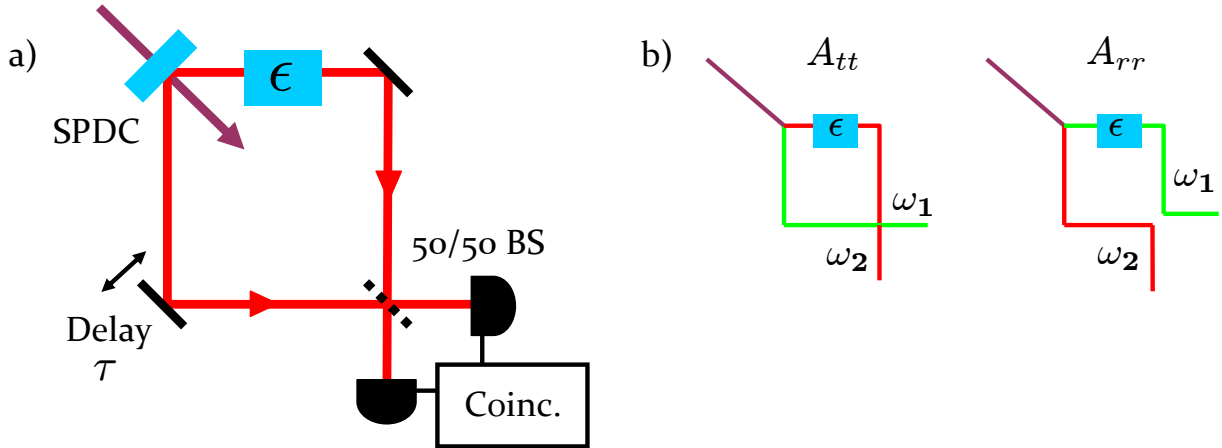


FIG. 1: Schematic of Hong-Ou-Mandel interferometry. a) Photon pairs, typically, though not necessarily, created via parametric down-conversion are emitted into two different spatial modes. One mode passes through a delay arm and the other passes through a sample. The photon pairs are recombined coherently at a 50/50 beamsplitter after the delay and samples. Photon counting detectors are placed in the output modes of the beamsplitter. The signal from the interferometer is the coincidence rate between those detectors as a function of the delay,  $\tau$ . b) There are two amplitudes leading to the detection of photons with frequencies,  $\omega_1$  and  $\omega_2$ . These amplitudes correspond to the Feynman paths shown, where either both photons are reflected at the beamsplitter or both photons are transmitted. The HOM signal is built up by the coherent addition of these amplitudes and the incoherent addition over all possible frequency pairs.

where we have used the fact that  $f(\omega_1, \omega_2) = f(\omega_2, \omega_1)$ . Integrating Eq. 4 with these amplitudes in yields

$$C(\tau) \propto 1 - \sqrt{\frac{2\sigma^2 + \sigma_c^2}{2\sigma^2 + \sigma_c^2 + \epsilon^2\sigma^4\sigma_c^2}} e^{-\frac{\tau^2\sigma^2(2\sigma^2 + \sigma_c^2)}{2(2\sigma^2 + \sigma_c^2 + \epsilon^2\sigma^4\sigma_c^2)}}. \quad (7)$$

From this expression, we see that the HOM signal is a Gaussian function of the time delay,  $\tau$ . The RMS width of the HOM signal,  $\tau_{HOM}$ ,

$$\tau_{HOM} = \frac{1}{\sigma} \sqrt{1 + \frac{\epsilon^2\sigma^4\sigma_c^2}{2\sigma^2 + \sigma_c^2}}. \quad (8)$$

It is useful to look at this expression in a few limits. If the dispersion of the material is 0, i.e.,  $\epsilon = 0$ , then  $\tau_{HOM} = \frac{1}{\sigma}$ . In other words, the width of the HOM dip is approximately the coherence time of the photon. If the photons have perfect frequency correlations, i.e.,  $\sigma_c = 0$ , then the width of the HOM dip is again given by the coherence time. In other words, if the photons have perfectly anticorrelated frequencies, then the width of the HOM dip in the presence of pure second-order dispersion is exactly the same as if there was no dispersion. This agrees with the conclusions of [4, 31]. Note that if there are no frequency correlations,  $\sigma_c \rightarrow \infty$ , then the dip is sensitive to the dispersion with  $\tau_{HOM} \rightarrow \frac{1}{\sigma} \sqrt{1 + \epsilon^2\sigma^4}$ .

Now we can consider the effect of imperfect correlations on the dispersion cancellation. Consider the limit where the photon correlations are strong, but imperfect,  $\sigma_c \ll \sigma$ . In this case, the width is given by

$$\tau_{HOM} \approx \frac{1}{\sigma} \sqrt{1 + \epsilon^2 \sigma^4 \frac{\sigma_c^2}{2\sigma^2}}. \quad (9)$$

Here it can be seen that the sensitivity to dispersion is reduced by a factor,  $\frac{\sigma_c^2}{2\sigma^2}$ . Assuming the photons are created by down-conversion, this reduction is roughly  $\frac{\tau_{photon}^2}{\tau_{pump}^2}$ , where  $\tau_{photon}$  is the coherence time of a down-conversion photon and  $\tau_{pump}$  is the coherence time of the pump laser. In other words the dispersion,  $\epsilon$ , is reduced to  $\epsilon \frac{\tau_{photon}}{\tau_{pump}}$  as a result of the frequency correlations. Note that even quantum dispersion cancellation is not perfect when the correlations are finite. However, in practice, it is straightforward to create down-converted photon bandwidths that are millions of times larger than the bandwidth of the pump laser [30, 33], thus the sensitivity to second-order dispersion can be reduced to a negligible level. One should keep in mind that automatic dispersion cancellation applies only to even-order dispersion; once the cubic (or third-order) dispersion becomes dominant, further reductions in sensitivity to second-order dispersion will not significantly aid signal quality.

## DISPERSION CANCELLATION IN CHIRPED-PULSE INTERFEROMETRY WITH FINITE CHIRP

Chirped-pulse interferometry (CPI) is a new technique designed to produce the metrological signature of the Hong-Ou-Mandel interferometer without the need for entanglement or single photons. A schematic of the chirped-pulse interferometer is shown in Fig. 2a. Two laser pulses are created with equal but opposite chirps; we refer to them as chirped (where the blue lags the red) and anti-chirped (where the red lags the blue). They are injected into different ports of the cross-correlator and recombined in a sum-frequency generation (SFG) after traveling through two different paths. A narrow spectrum of the SFG is detected on a square-law detector. The intensity of the SFG as a function of delay is the CPI signal.

The nonlinear detection in CPI relies on sum-frequency generation, a second-order nonlinear process. In such processes, the nonlinear polarization,  $P_{NL}(t)$  in the medium depends on the product of the two driving fields:

$$P_{NL}(t) \propto \chi^{(2)} E_1(t) E_2(t) \quad (10)$$

This nonlinear polarization can reradiate light at frequencies corresponding to its frequency components. We make the assumption that the nonlinearity is fast so that  $\chi^{(2)}$  can be treated as a constant. We will also make the assumption that the driving fields are not depleted and that perfect phase-matching over all driving frequencies is achieved. We make the approximation that the radiated field is proportional to the polarization and the slowly varying amplitude approximation [34] and rewrite Eq. 10 to obtain an expression for the SFG electric field amplitude in the frequency domain,

$$E_3(\omega) \approx \int d\omega' E_1(\omega') E_2(\omega - \omega') \quad (11)$$

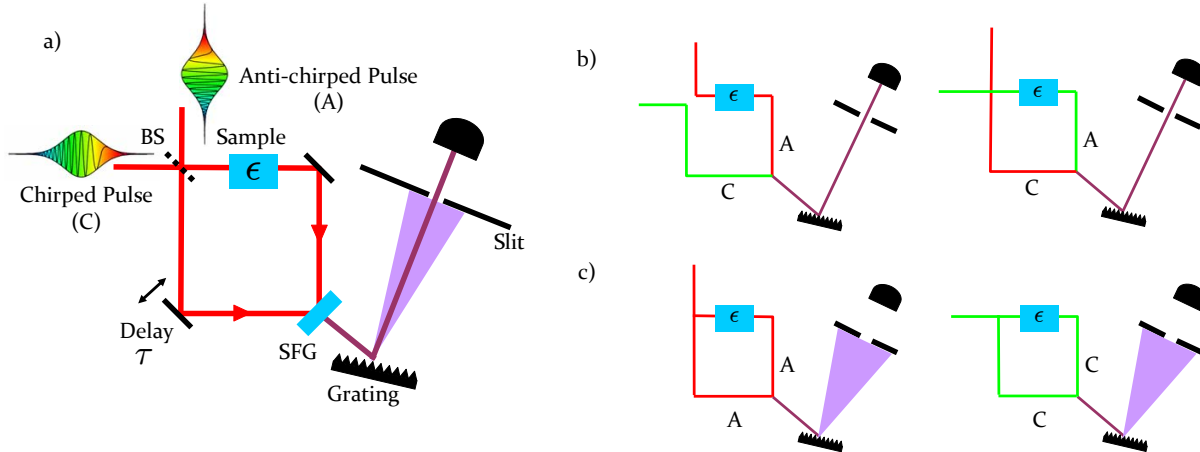


FIG. 2: Schematic of chirped-pulse interferometry. a) Chirped-pulse interferometer. A pair of oppositely-chirped laser pulses are combined coherently at a 50/50 beamsplitter. A variable delay arm is placed in one of the modes (a reference) while a sample is placed in the other arm. (In this paper, the sample will be assumed to introduce a pure quadratic phase,  $\phi(\omega) = \epsilon(\omega - \omega_0)^2$ ). After the sample, the light in the reference and sample arms are used to create sum-frequency generation (SFG) in a nonlinear material. The narrow band of the SFG created by the cross-correlation of the chirped and anti-chirped beams is detected with a square-law detector. The detected intensity as a function of the delay,  $\tau$ , is the CPI signal. b) The two Feynman paths leading to narrow-band SFG. These involve contributions where the chirped pulse passes through the sample arm and the anti-chirped pulse passes through the reference or vice versa. c) The two paths leading to broad band SFG. These contributions are from the autocorrelations where the chirped (or antichirped) pulses alone create SFG. Contributions to the signal from these processes can be almost entirely removed from spectral filtering when the pulses are stretched to many times their transform-limited duration. In the calculations presented here, we ignore these processes.

The positive frequency electric field amplitudes for a linearly chirped pulse can be written,

$$E(\omega; A) = E_0 e^{\frac{(\omega - \omega_0)^2}{2\sigma^2}} e^{iA(\omega - \omega_0)^2}, \quad (12)$$

where  $\sigma$  is the RMS bandwidth of the field and  $A$  determines the strength and sign of the chirp. CPI relies on strong frequency correlations which come from chirping the pulses to many times their transform-limited pulse duration, i.e.,  $A \gg \frac{1}{\sigma^2}$ .

We overlap the oppositely chirped pulses on the input beam splitter of our interferometer. In one arm of the interferometer the pulses experience a relative time delay  $\tau$  with respect to the other arm. The field in this delay arm can be written as:

$$E_1(\omega, \tau) = [E(\omega; A) + E(\omega; -A)] e^{i\tau\omega}. \quad (13)$$

In the second arm of the interferometer the light passes through a sample with purely quadratic dispersion (i.e., we ignore the group delay which just leads to an offset of the interference from  $\tau = 0$ ). The phase imparted by the material for our model is again,  $\phi(\omega) = \epsilon(\omega - \omega_0)^2$ . Thus, we can write the field after the dispersive sample as

$$E_2(\omega, \tau) = [E(\omega; A) - E(\omega; -A)] e^{i\epsilon(\omega - \omega_0)^2}, \quad (14)$$

where the minus sign reflects the  $\pi$  phase shift acquired at the input beam splitter.

It has been shown that pairs of strongly oppositely-chirped laser pulses produce very narrow band sum-frequency generation [35]. In the following calculation, we make the assumption that the laser pulses have large chirp, such that the pulse durations is much longer than the coherence time (or transform limited pulse duration) and that the difference in the delay between the two paths in the interferometer are small compared with the chirped pulse duration. In this limit, the SFG from the cross-correlation (Fig. 2b) will have much narrower bandwidth than the autocorrelation (Fig. 2c) and thus can be selected using spectral filtering allowing us to ignore the contribution from the autocorrelation. In this case, the CPI signal will be given by

$$E_3(\omega, \tau) \approx \int d\omega' [E(\omega'; -A)E(\omega - \omega'; A) - E(\omega'; A)E(\omega - \omega'; -A)] e^{i\tau\omega' + i\epsilon(\omega - \omega' - \omega_0)^2} \quad (15)$$

The total SFG power detected as a function of the time delay  $\tau$  is given by,

$$\begin{aligned} I_{SFG}(\tau) &\propto \int d\omega |E_3(\omega, \tau)|^2 \\ &\propto \Lambda_+ e^{-\frac{\tau^2}{2\tau_+^2}} + \Lambda_- e^{-\frac{\tau^2}{2\tau_-^2}} - \Lambda_c \cos[\zeta - \alpha\tau^2] e^{-\frac{\tau^2}{2\tau_{cpi}^2}}, \end{aligned} \quad (16)$$

with the following definitions,

$$\begin{aligned} \Lambda_{\pm} &= \frac{(2\pi^5)^{\frac{1}{2}} \sigma}{[1+2(2A^2 \pm 2A\epsilon + \epsilon^2)\sigma^4]^{\frac{1}{2}}}, & \Lambda_c &= \frac{(2\pi^5)^{\frac{1}{2}} \sigma}{\{16A^2\epsilon^4\sigma^{12} + [1+2(2A^2 + \epsilon^2)\sigma^4]^2\}^{\frac{1}{4}}}, \\ \zeta &= \frac{1}{2} \arctan \left[ \frac{4A\epsilon^2\sigma^6}{1+2(2A^2 + \epsilon^2)\sigma^4} \right], & \alpha &= \frac{2A\epsilon^2\sigma^8}{4A^2\sigma^4 + (1+2\epsilon^2\sigma^4)^2}, \\ \tau_{\pm} &= \left[ \frac{1}{\sigma^2} + 2(2A^2 \pm 2A\epsilon + \epsilon^2)\sigma^2 \right]^{\frac{1}{2}} & \tau_{cpi} &= \frac{1}{\sigma} \left[ \frac{4A^2\sigma^4 + (1+2\epsilon^2\sigma^4)^2}{1+2(2A^2 + \epsilon^2)\sigma^4} \right]^{\frac{1}{2}}. \end{aligned} \quad (17)$$

This are rather complicated expressions, so it is worth examining the terms in a little detail. The first two terms in Eq. 16 are nearly identical when  $A \gg \epsilon$  and describe a broad Gaussian signal with the time duration of the chirped pulses. The last term describes the interference dip. If the chirp is large compared to the dispersion, the cosine will be  $\approx 1$  where the CPI dip occurs. Outside of this limit the cosine term will start to modulate the interference term, and the phase offset  $\zeta$  will start to reduce the visibility of the CPI dip.

The RMS width of the CPI dip is given by the expression for  $\tau_{cpi}$  which can be written

$$\tau_{cpi} = \frac{1}{\sigma} \sqrt{1 + \epsilon^2\sigma^4 \left( \frac{2 + 4\epsilon^2\sigma^4}{1 + 4A^2\sigma^4 + 2\epsilon^2\sigma^4} \right)}, \quad (18)$$

which has a similar form to Eq. 9. When the chirp is larger than the dispersion, we can simplify this expression to,

$$\tau_{cpi} = \frac{1}{\sigma} \sqrt{1 + \epsilon^2\sigma^4 \left( \frac{2 + 4\epsilon^2\sigma^4}{1 + 4A^2\sigma^4} \right)}. \quad (19)$$

The dispersion in CPI is reduced by a small factor,  $\frac{2+4\epsilon^2\sigma^4}{1+4A^2\sigma^4}$ . This ratio is approximately the ratio  $\frac{\tau_{\epsilon}^2}{\tau_{chirp}^2}$ , where  $\tau_{\epsilon}$  is the time duration of a transform-limited pulse subjected to the

dispersive phase,  $\phi(\omega)$ , and  $\tau_{chirp}$  is the time duration of the chirped pulse. Here, in strong analogy with the quantum case, we can view the dispersion as having been reduced from  $\epsilon$  to  $\epsilon \frac{\tau_\epsilon}{\tau_{chirp}}$ . Thus as the chirp pulse duration goes to infinity, the dispersion cancellation becomes perfect. With grating-based stretchers and compressors, femtosecond pulses can easily be stretched [36] by a factor of 1000, thus reducing the sensitivity to the typically dominant second-order dispersion by two to three orders of magnitude.

## CONCLUSIONS

We have presented models describing the entangled photons in Hong-Ou-Mandel interferometry and the laser pulses in chirped-pulse interferometry which allow for varying degrees of correlation. In the case of perfect correlations, both HOM and CPI exhibit complete insensitivity to second-order dispersion [37]. When imperfect correlations are considered, neither interferometer completely cancels second-order dispersion, but the effective second-order dispersion can be reduced significantly. In the HOM interferometer, the second-order dispersion is reduced by roughly the ratio of the down-converted photon coherence time to the pump coherence time. In CPI, the dispersion is reduced by the ratio of the time duration of a transform-limited pulse subjected to the dispersive phase to the chirped pulse duration. It is straightforward in practice to make both of these ratios small, although it is certainly easier to make the quantum ratio very small ( $< 10^{-6}$ ). For thick enough materials or extremely large bandwidth, odd-order dispersion terms, which are not cancelled, will dominate the signal after which further reduction in the sensitivity to second-order dispersion will not help signal quality.

Our results constitute simple rules of thumb for estimating the maximum tolerable level of dispersion in the HOM interferometer and CPI for a given strength of correlations. These considerations will be important in designing optical technologies which exploit automatic dispersion cancellation with either quantum or classical resources.

The authors thank Grant Salton, Kostadinka Bizheva, Donna Strickland, and Gregor Weihs for valuable discussions. This work was supported by National Sciences and Engineering Research Council of Canada, the Canadian Foundation for Innovation, Ontario Centres of Excellence, and an Ontario Ministry of Research and Innovation Early Researcher Award. R.K. is partially funded by the Institute for Quantum Computing; D.B. is funded by a Mike and Ophelia Lazaridis Scholarship; J.L. is partially funded by the Bell Family Fund.

---

\* Electronic address: kresch@iqc.ca

- [1] Michelson, A.A. and Morley, E.W., “On the Relative Motion of the Earth and the Luminiferous Ether”, *American Journal of Science* 34, 333-345 (1887).
- [2] Abbott, B. et al., “Upper limits on a stochastic background of gravitational waves,” *Phys. Rev. Lett.* 95, 221101 (2005).
- [3] Steinberg, A.M., Kwiat, P.G. and Chiao, R.Y., “Dispersion cancellation in a measurement of the single-photon propagation velocity in glass,” *Phys. Rev. Lett.* 68, 2421-2424 (1992).
- [4] Steinberg, A.M., Kwiat, P.G. and Chiao, R.Y., “Dispersion cancellation and high-resolution time measurements in a fourth-order optical interferometer,” *Phys. Rev. A* 45, 6659-6665 (1992).



- [5] Franson, J.D., “Nonlocal cancellation of dispersion,” *Phys. Rev. A* 45, 3126-3132 (1992).
- [6] Hong, C.K., Ou, Z.Y., and Mandel, L., “Measurement of subpicosecond time intervals between two photons by interference,” *Phys. Rev. Lett.* 59, 2044-2046 (1987).
- [7] Franson, J.D., “Bell inequality for position and time,” *Phys. Rev. Lett.* 62, 2205-2208 (1989).
- [8] Ou, Z.Y., Zou, X.Y., Wang, L.J., and Mandel, L., “Observation of nonlocal interference in separated photon channels,” *Phys. Rev. Lett.* 65, 321-324 (1990).
- [9] Pittman, T.B., Shih, V.H., Strekalov, D.V., and Sergienko, A.V., “Optical imaging by means of two-photon quantum entanglement,” *Phys. Rev. A* 52, R3429-R3432 (1995).
- [10] Strekalov, D.V., Sergienko, A.V., Klyshko, D.N., and Shih, Y.H., “Observation of Two-Photon Ghost Interference and Diffraction,” *Phys. Rev. Lett.* 74, 3600-3603 (1995).
- [11] Lee, H., Kok, P., and Dowling, J.P., “A quantum Rosetta stone for interferometry,” *J. Mod. Opt.* 49, 2325-2338 (2002).
- [12] Giovannetti, V., Lloyd, S. and Maccone, L., “Quantum-Enhanced Measurements: Beating the Standard Quantum Limit,” *Science* 306, 1330-1336 (2004).
- [13] M. W. Mitchell, J. S. Lundeen, and A. M. Steinberg, “Super-resolving phase measurements with a multiphoton entangled state,” *Nature* 429, 161-164 (2004).
- [14] P. Walther, J.-W. Pan, M. Aspelmeyer, R. Ursin, S. Gasparoni, and A. Zeilinger, “De Broglie wavelength of a non-local four-photon state,” *Nature* 429, 158-161 (2004).
- [15] B. Yurke, “Input states for enhancement of fermion interferometer sensitivity,” *Phys. Rev. Lett.* 56, 1515-1517 (1986).
- [16] J. G. Rarity, P. R. Tapster, E. Jakeman, T. Larchuk, R. A. Campos, M. C. Teich, and B. E. A. Saleh, “2-photon interference in a Mach-Zehnder interferometer,” *Phys. Rev. Lett.* 65, 1348-1351 (1990).
- [17] R. S. Bennink, S. J. Bentley, and R.W. Boyd, “‘Two-photon’ coincidence imaging with a classical source,” *Phys. Rev. Lett.* 89, 113601 (2002).
- [18] F. Ferri, D. Magatti, A. Gatti, M. Bache, E. Brambilla, and L.A. Lugiato, “High-resolution ghost image and ghost diffraction experiments with thermal light,” *Phys. Rev. Lett.* 94, 183602 (2005).
- [19] K.J. Resch, P. Puvanathan, J.S. Lundeen, M.W. Mitchell, and K. Bizheva, “Classical dispersion-cancellation interferometry,” *Opt. Express* 15, 8797-8804 (2007).
- [20] K.J. Resch, P. Puvanathan, K. Bizheva, M. Mitchell, and J.S. Lundeen, “White-light interferometer automatically cancels dispersion,” *Laser Focus World* 43, 85-89 (2007).
- [21] R. Kaltenbaek, J. Lavoie, D. N. Biggerstaff, and K. J. Resch, “Quantum-inspired interferometry with chirped laser pulses,” *Nature Phys.* 4, 864-868 (2008).
- [22] J. Lavoie, R. Kaltenbaek, and K. J. Resch, “Quantum-optical coherence tomography with classical light,” *Opt. Express* 17, 3818-3825 (2009).
- [23] K.J. Resch, K.L. Pregnell, R. Prevedel, A. Gilchrist, G.J. Pryde, J.L. O’Brien, and A.G. White, “Time-reversal and super-resolving phase measurements,” *Phys. Rev. Lett.* 98, 223601 (2007).
- [24] R. Kaltenbaek, J. Lavoie, and K. J. Resch, “Classical analogues of two-photon quantum interference,” *Phys. Rev. Lett.* 102, 243601 (2009).
- [25] K.F. Lee and J.E. Thomas, “Experimental Simulation of Two-Particle Quantum Entanglement using Classical Fields,” *Phys. Rev. Lett.* 88, 097902 (2002).
- [26] K.F. Lee and J.E. Thomas, “Entanglement with classical fields,” *Phys. Rev. A* 69, 052311 (2004).
- [27] K.F. Lee, “Observation of bipartite correlations using coherent light for optical communication,” *Optics Letters* 34, 1099-1101 (2009).

- [28] B.I. Erkmen and J.H. Shapiro, “Phase-conjugate optical coherence tomography,” *Phys. Rev. A* 74, 041601 (2006).
- [29] K. Banaszek, A.S. Radunsky, and I.A. Walmsley, “Blind dispersion compensation for optical coherence tomography,” *Opt. Commun.* 269, 152-155 (2007).
- [30] M.B. Nasr, S. Carrasco, B.E.A. Saleh, A.V. Sergienko, M.C. Teich, J.P. Torres, L. Torner, D.S. Hum, M.M. Fejer, “Ultrabroadband biphotons generated via chirped quasi-phase-matched optical parametric down-conversion” *Phys. Rev. Lett.* 100, 199903 (2008).
- [31] A. F. Abouraddy, M. B. Nasr, B. E. A. Saleh, A. V. Sergienko, and M. C. Teich, “Quantum-optical coherence tomography with dispersion cancellation,” *Phys. Rev. A* 65, 053817 (2002).
- [32] M.B. Nasr, B.E.A. Saleh, A.V. Sergienko, and M.C. Teich, “Demonstration of dispersion-canceled quantum-optical coherence tomography,” *Phys. Rev. Lett.* 91, 083601 (2003).
- [33] P.G. Kwiat, A.M. Steinberg, and R.Y. Chiao, “High-visibility interference in a Bell-inequality experiment for energy and time,” *Phys. Rev. A* 47, R2472-R2475 (1993).
- [34] Boyd, R.W., [Nonlinear Optics Third Edition], Academic Press, New York p.76 (2008).
- [35] F. Raoult, A. C. L. Boscheron, D. Husson, C. Sauteret, A. Modena, V. Malka, F. Dorchies, and A. Migus, “Efficient generation of narrow-bandwidth picosecond pulses by frequency doubling of femtosecond chirped pulses,” *Opt. Lett.* 23, 1117-1119 (1998).
- [36] M. Pessot, P. Maine and G. Mourou, “1000 times expansion compression of optical pulses for chirped pulse amplification,” *Opt. Commun.* 62, 419-421 (1987).
- [37] In Ref. [21], we showed that CPI is insensitive to all even orders of dispersion in the case of perfect correlation.